Modeling Energy Dissipation and De-tumbling of a Defunct Satellite Using a Finite Element Method

Ryotaro Sakamoto, Daniel J. Scheeres
University of Colorado Boulder, Boulder, CO

ABSTRACT

The combination of finite element methods and flexible body theory are used to model energy dissipation and the de-tumbling process of defunct satellites from a complex rotation state. Several factors can cause the damping out of excess energy in a spinning body in space. One of that is a deformation of flexible components. We model deformation using a finite element analysis and generate a time varying inertia matrix which drives the bodys rotational dynamics. Energy dissipation and spin rate transition are observed from this approach. This analysis will contribute to the precise modeling of non-uniformly rotating debris and defunct satellites.

1. INTRODUCTION

There are several causes which can cause the spin rate change of a space object, both internal and external effects. The Yarkovsky-OKeefe-Radizievskii-Paddack (YORP) effect led by solar radiation pressure is considered as one cause of changes in the rotational states of defunct geosynchronous earth orbit (GEO) satellites. For example, the transition of the rotational rates has been predicted and observed in the GOES 8 satellite [1] as shown in Fig. 1. This effect does not only affect defunct satellites such as GOES 8 satellite, as the rotational rates of small asteroids are also changed by the YORP effect [6]. To understand the mechanism of the transition of satellite spin states, internal energy dissipation is a key component. In ideal situation, the kinetic energy is conserved without any additional torque for rigid body dynamics. But in real life, friction between structural components or sloshing of internal liquid are considered as reasons for dissipation in space [5, 3]. In this study, the deformation is taken into account as the primary cause to internal energy dissipation and spin rate transition of analysis model.

Finite element analysis calculates the deformational behavior of satellite model based on the damping equation, given

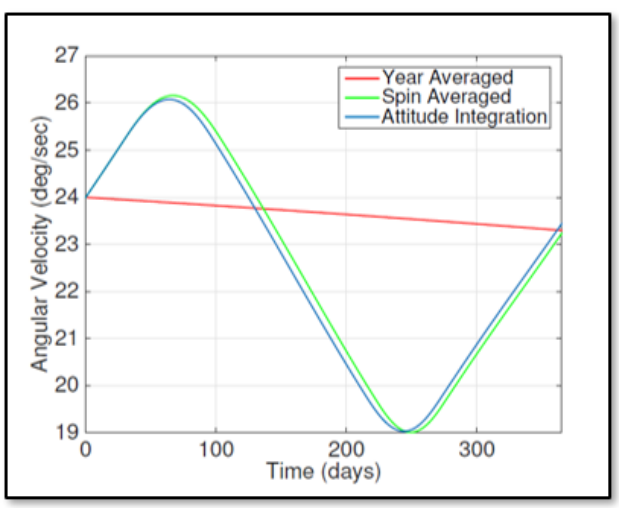

Fig. 1: Spin Rate Change of GOES 8

a driving acceleration. Due to the fluctuation of flexible components, the body axis is affected as it is tumbling at

the same time. This causes the inertia matrix and its products of inertia to be updated due to the deformation results. Then, flexible body equation, which is based on the Euler equation, provides us an update of the spin state. When combined, these processes can model the interaction of deformation and the spin rate transition of rotational dynamics. As a tumbling satellite loses energy, the state of the rotational rate approaches rotation along its maximum moment of inertia. In term of the three-dimensional dynamics, rotational rate along its maximum momentum inertia goes to a value based on minimum energy theory with the other rotational rates going to zero. Our goal is to find the relationship between the rate of energy dissipation and material properties for spinning defunct satellites and debris in general. Our simulation model is comprised of solar array panels and body component using a finite element model. The entire simulation results are compared with a simple rigid body dynamic with varying dynamical properties such as the damping ratio and spin rates. Then the relaxation time of spin rates transitions are estimated to enable our approach to be effectively used to analyze a wider range of satellites and debris objects.

2. MODELING FOR INVESTIGATION

2.1 Analysis model with FEM

To evaluate deformation and damping of the system, we develop the three dimensional analysis model based on the Finite Element Method (FEM) as shown in Figs. 2 and 3. Fig. 2 shows overview of the analysis model with FEM software, which verifies the structural behaviors. Fig.3 shows the details of one and setups for Matlab simulation. This typical satellite model is composed of a rigid main component and flexible two SAP, which can simulate the interaction of a rigid component and flexible components. To cause fluctuation behavior largely, joint element motivated by beams are introduced between each SAP component. The total model size of satellite is 1.0 [m] (X direction) $\times$ 5.0 [m] (Y direction) $\times$ 0.5 [m] (Z direction).

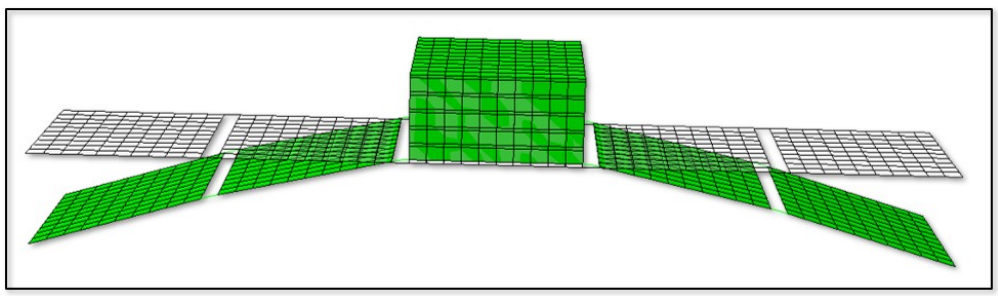

Fig. 2: Analysis Model (FEM software)

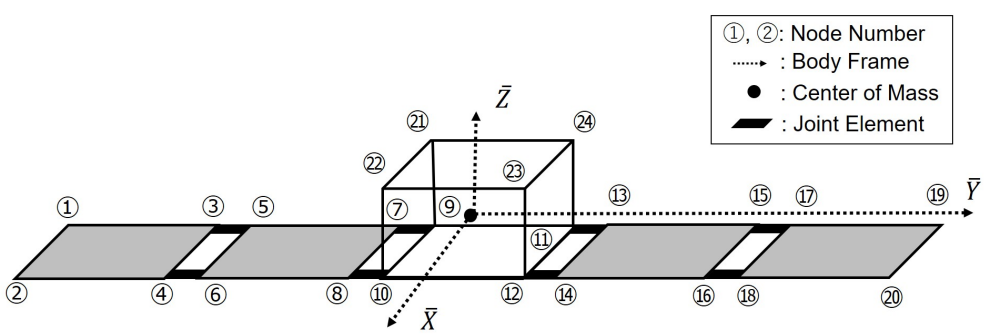

Fig. 3: Analysis Model (Matlab)

2.2 Dynamics model

The damping equation (Eq. 1) is used to investigate the dynamical behavior of the structure.

$$M\ddot{X} + C\dot{X} + KX = \vec{f}(t) \tag{1}$$

where M is the mass matrix, C is the damping matrix, K is the stiffness matrix, and $\vec{f}(t)$ is the excitation force. For numerical efficiency, the mass matrix is taken as a lumped mass matrix [4]. For the damping matrix, we defined as following,

$$[C] = \alpha[M] + \beta[K] \tag{2}$$

α and β are coefficients and given by following.

$$\alpha = \zeta \frac{2w_i w_j}{w_i + w_j},\ \beta = \zeta \frac{2}{w_i + w_j} \tag{3}$$

where ζ is a damping ratio and w_i and w_j are i^{th} and j^{th} natural frequencies of the system [2]. We assume the damping ratio ζ is same at the ith and j^{th} mode frequencies for the simplicity. Damping ratio make a differential behavior of our system, the variation of ζ and effects are explored in our simulation.

2.3 Rotational Dynamics

In order to simulate the tumbling model, a three dimensional acceleration matrix in the body frame is developed. This acceleration matrix is applied into Eq. 1 as an excitation force. An arbitrary angular velocity $\vec{\omega}$, is defined the angular velocity of the body frame relative to the inertial frame. Then, the acceleration matrix in the body frame is given by

$$\vec{f}(t) = [\omega^2 I_{3\times3} - \vec{\omega}\vec{\omega} - \tilde{\dot{\vec{\omega}}}] \cdot \vec{r} \tag{4}$$

where $\sim$ denotes a skew-symmetric matrix. Fig. 4 illustrates a position vector $\vec{r}$ of node 1 in the body frame. Since FEM simulation provides the displacements vector $\vec{d}'s$ from the original position, $\vec{r}$ in the body frame is defined by the node position plus each displacement vector of all nodes.

For our initial analysis, we use a basic angular velocity vector that models the rotational dynamics is given by Eq. 5.

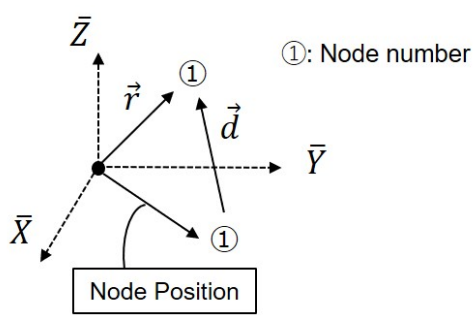

Fig. 4: Position Vector with Displacement Vector

$$\vec{\omega}(t) = \begin{bmatrix} \omega_\perp \cos(\omega_0 \times t) \\ \omega_\perp \sin(\omega_0 \times t) \\ \omega_0 \end{bmatrix},\ \omega_\perp = F \times \omega_0 \tag{5}$$

where ω_0 is a spin rate along $\bar{Z}$ axis component in the body frame, and $\omega_\perp$ is the perpendicular spin rates with the $\bar{Z}$ axis. F is the ratio of a pure spin and tumbling. Based on Eqs. 4 and 5, the three dimensional acceleration matrix is defined by

$$\vec{f}(t) = \begin{bmatrix} \omega^2 - \omega_\perp^2 \cos^2(\omega_0 t) & -\omega_\perp^2 \sin(\omega_0 t)\cos(\omega_0 t) & -\omega_\perp \omega_0 \cos(\omega_0 t) \\ -\omega_\perp^2 \sin(\omega_0 t)\cos(\omega_0 t) & \omega^2 - \omega_\perp^2 \sin^2(\omega_0 t) & -\omega_\perp \omega_0 \sin(\omega_0 t) \\ -\omega_\perp \omega_0 \cos(\omega_0 t) & -\omega_\perp \omega_0 \sin(\omega_0 t) & \omega^2 - \omega_0^2 \end{bmatrix} \vec{r} \tag{6}$$

where, $\omega^2 = \omega_0^2 + \omega_\perp^2$.

2.4 Flexible Body Dynamics

For rigid body dynamics, the equation of motion are defined as

$$[I_0]\dot{\vec{\omega}} = -\tilde{\vec{\omega}}[I_0]\vec{\omega} \tag{7}$$

where $[I_0]$ is a constant inertia matrix. For this study, the inertia matrix written as $[I(t)]$, which denotes that the inertia matrix is time varying and is treated as having flexible body dynamics. If the time derivative of the inertia matrix $[\dot{I(t)}]$ is also considered, the equation of flexible body dynamics is given by

$$[I(t)]\dot{\vec{\omega}} = -\tilde{\vec{\omega}}[I(t)]\vec{\omega} - [\dot{I(t)}]\vec{\omega} \tag{8}$$

Generally, the inertia matrix for a rigid body using our lumped mass model is given by,

$$[I_0] = -\sum_{i=1}^{N} m_i \tilde{\vec{r}}\tilde{\vec{r}} \tag{9}$$

Then the time derivative of Eq. 9 is,

$$[\dot{I(t)}] = -\left(\sum_{i=1}^{N} m_i \dot{\tilde{\vec{r}}}\tilde{\vec{r}} + \sum_{i=1}^{N} m_i \tilde{\vec{r}}\dot{\tilde{\vec{r}}}\right) \tag{10}$$

By combined with the information of displacement from the FEM simulation, the deformation can be applied as the flexible variable to the body dynamics.

3. SIMULATION SETUPS

In the following simulations, first we discuss how deformation affects internal energy dissipation and spin rate transition of the tumbling model. Using the our findings, we leverage them for estimation of relaxation times of spinning with the change of damping ratio and spin rates for the following section.

3.1 Simulation Sequence

Fig. 5 shows a simulation sequence for the combination of the FEM dynamics with the flexible body theory. Dynamic state is composed of FEM and flexible body variables. MRP is also considered to confirm the inertial parameters. In total, three equations are integrated simultaneously. During this simulation, spin rate, the inertia matrix $[I(t)]$ and its derivative $[\dot{I(t)}]$ are updated each time step.

3.2 Rigid and Flexible Comparison

Based on the parameters as shown in Tab. 1, simulation is conducted. For the simulation simplicity, w_i and w_j is set as 0.1 in Eq. 3. and F is 1.0 in Eq. 5. Fig. 6 shows the time history of the angular velocities in the body frame. Here blue lines show simple rigid body dynamics with a constant inertia matrix, and the red lines show the flexible body dynamics. For the rigid body, spin states of all axes do not change. However, for the flexible body case, ω_x and ω_y are damping out to zero, and ω_z approaches a particular value as time goes on. The magnitude of the angular momentum in the inertial frame, as shown in Fig. 8, is observed as a conserved quantity. Fig.9 shows the kinetic rotational energies of the rigid and the flexible body dynamics defined as $\vec{\omega}^T I \vec{\omega}$. The nominal value is constant but the blue line is decreasing forward to minimum energy state E_{min} along with the exponential function.

Table 1: Simulation Parameters of Energy Dissipation

Damping	ζ = 0.1,	$w_i = w_j = 0.1$
Spinning	F = 1.0	$\frac{2\pi}{360}$[rad/sec]

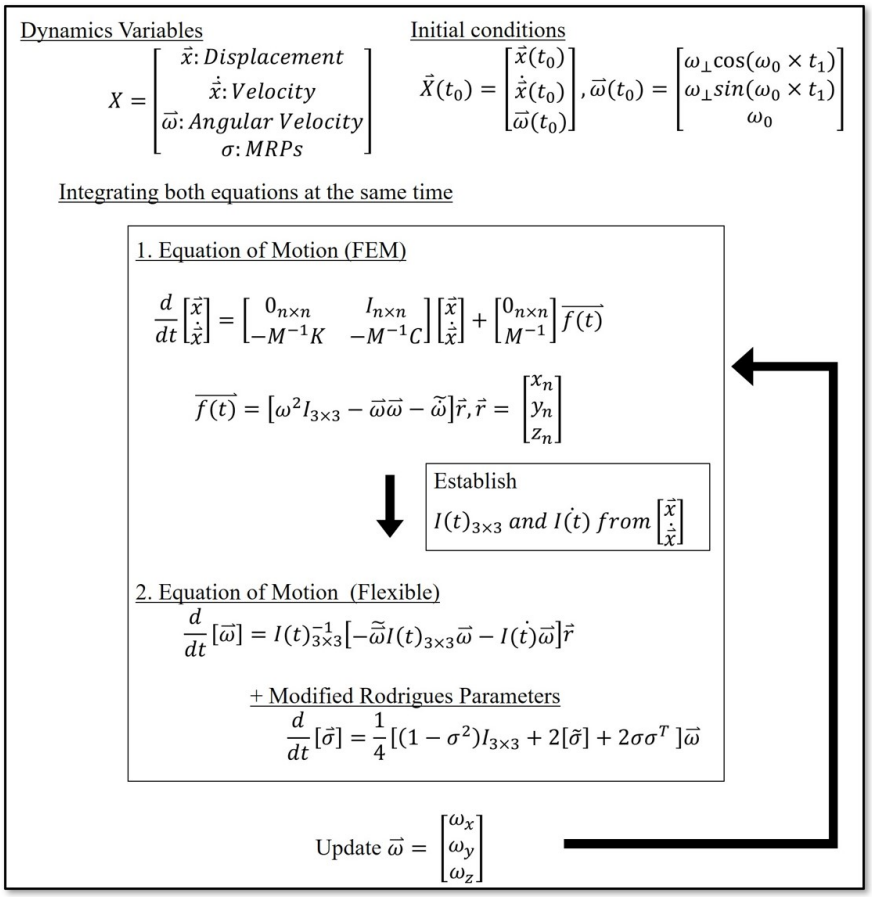

Fig. 5: Simulation Sequence

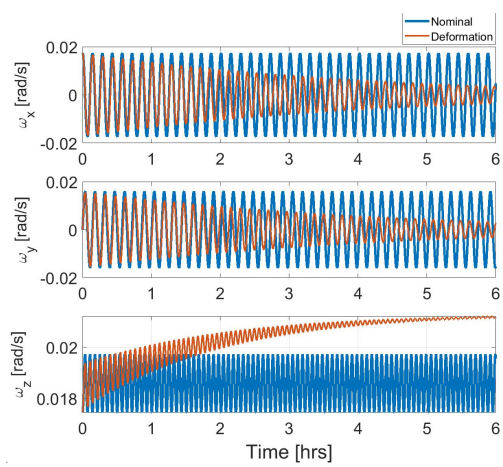

Fig. 6: Angular Velocities $\vec{\omega}$

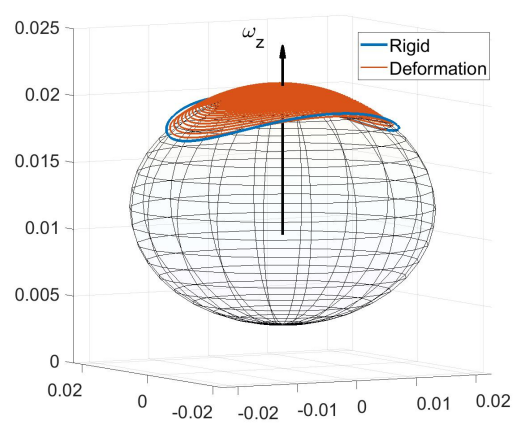

Fig. 7: Sphere of $\vec{\omega}$

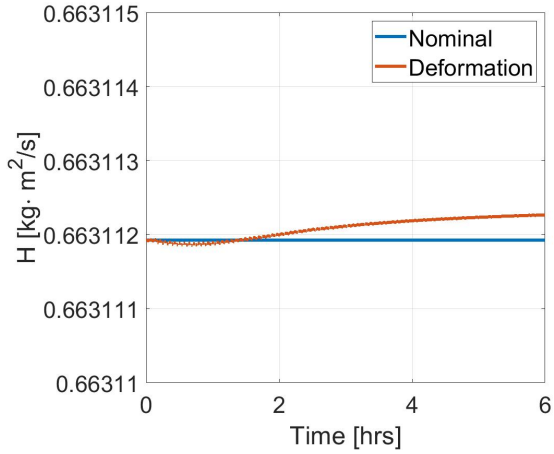

Fig. 8: Angular Momentum $|\vec{H}|$

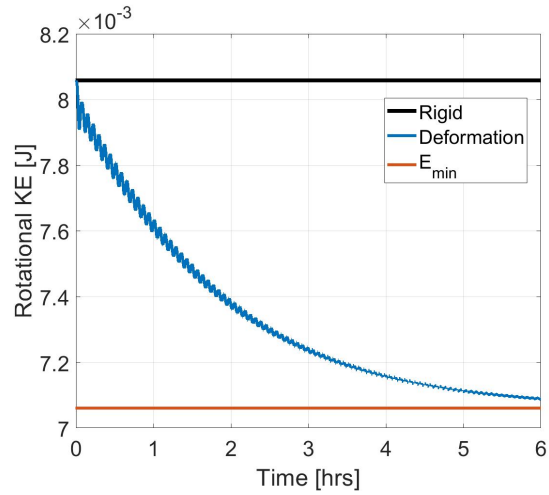

Fig. 9: Rotational Energy T_{rot}

4. SIMULATIONAL ANALYSIS

4.1 Estimation for Energy Loss

As we demonstrated above section, the energy dissipation is along the exponential function. At the same time, the relaxation time can be estimated along the exponential function as well. To make estimation approach more concrete ways, we explore the variation of tumbling conditions. The most critical value to make behavior change is the damping ratio (ζ) in this system. Therefore, we investigate the relationship between the damping ratio and energy decay curves. The range of the damping ratio is set as its reasonable simulation time. Next, we explored the relationship between spin rate and shape of energy decay curves. Simulation parameters are summarized in Tab. 2.

Table 2: Simulation Parameters under Conditions

Variation	ζ	ω_0 [rad/sec]
Damping Ratio (ζ)	$0.01 \sim 0.1$	$\frac{2\pi}{360}$
Spin Rate (ω_0)	$0.01 \sim 0.1$	$\frac{2\pi}{180}, \frac{2\pi}{360}, \frac{2\pi}{540}$

4.2 Variation of Damping Ratio and Spin Rate

Fig. 10 shows the variation of the energy decay curves with change in the damping ratio with $\omega_0 = \frac{2\pi}{360}$. As shown in this figure, energy decay with a weaker damping ($\zeta = 0.01$) needs a longer relaxation time. Also, strong damping makes energy decay sharp ($\zeta = 0.1$). Fig. 11 shows more general shape with applying $Time \times \zeta$ on the vertical axis. Here, we can estimate the relaxation time along the exponential function shown as Fig. 12. Fig. 13 shows the plots of energy state with a changing damping ratio and different spin rate as previous condition. Even different spin rates and damping ratios as shown in Tab. 2, the energy decay curves are similar shape and the relaxation time can be predicted.

5. CONCLUSION

By combing FEM dynamics, flexible body, and rotational dynamics, we investigated the relationship between de-tumbling and internal energy dissipation. In section 3 and 4, we presented the numerical results of the patterns of the spin rate and damping ratio. Using the exponential function, we demonstrated the possibility to predict the relaxation time. We believe that these modeling techniques will be useful in studying the de-tumbling satellites or asteroids. As we discussed in the introduction, by comparing our computed spin rate transitions with observation data for the tumbling satellite GOES-8 [1], we will develop estimates of what appropriate level of dissipation should be used in various situations.

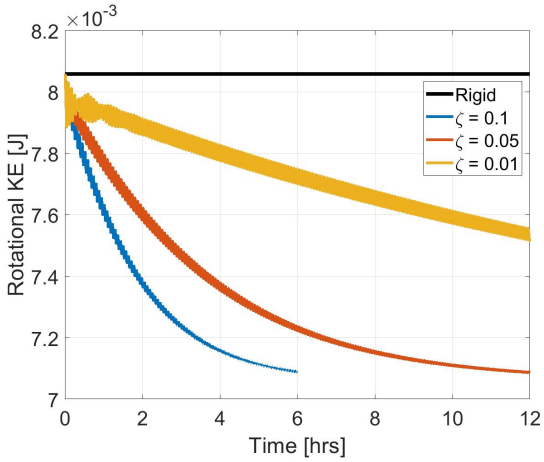

Fig. 10: Energy Decay with $\omega_0 = \frac{2\pi}{360}$

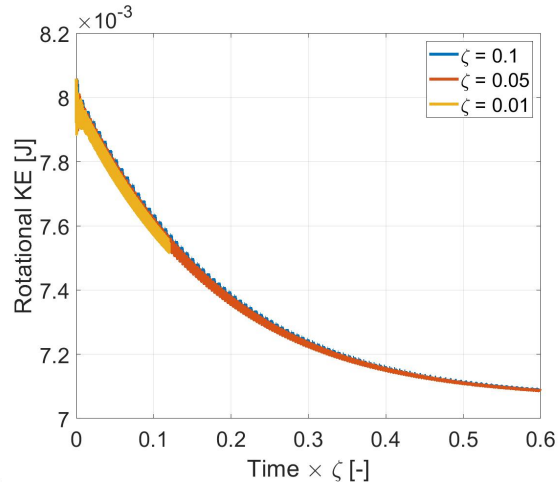

Fig. 11: Energy Decay with Time $\times\zeta$

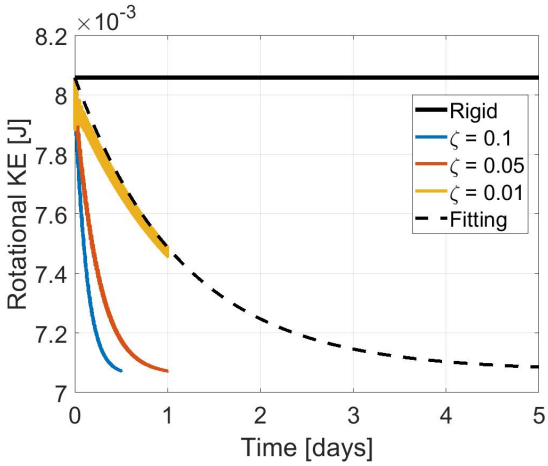

Fig. 12: Estimation of Energy Decay

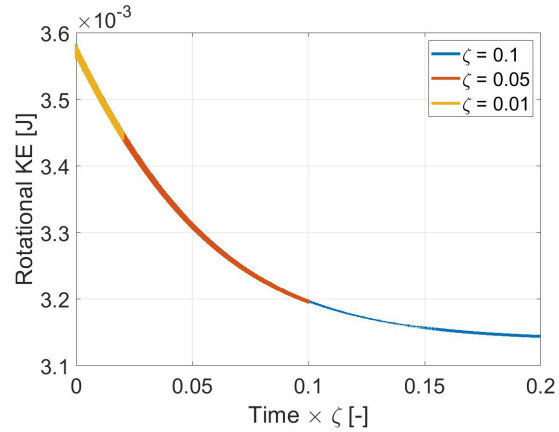

Fig. 13: Estimation of Decay with $\omega_0 = \frac{2\pi}{540}$

6. REFERENCES

[1] Antonella A Albuja, Daniel J Scheeres, and Jay W McMahon. Evolution of angular velocity for defunct satellites as a result of yorp: An initial study. *Advances in Space Research*, 56(2):237–251, 2015.

[2] Klaus Jurgen Bathe. *Finite element procedures*. Klaus-Jurgen Bathe, 2006.

[3] M Chiba and H Magata. Influence of liquid sloshing on dynamics of flexible space structures. *Journal of Sound and Vibration*, 401:1–22, 2017.

[4] SS Deshpande, SR Rawat, NP Bandewar, and MY Soman. Consistent and lumped mass matrices in dynamics and their impact on finite element analysis results. *Intern. J. of Mechanical Engineering and Technology (IJMET)*, 7(2):135–147, 2016.

[5] Yasushi Kojima, Shigemune Taniwaki, and Yoshiaki Okami. Dynamic simulation of stick–slip motion of a flexible solar array. *Control Engineering Practice*, 16(6):724–735, 2008.

[6] Stephen C Lowry, Alan Fitzsimmons, Petr Pravec, David Vokrouhlickỳ, Hermann Boehnhardt, Patrick A Taylor, Jean-Luc Margot, Adrian Galád, Mike Irwin, Jonathan Irwin, and Peter Kusnirák. Direct detection of the asteroidal yorp effect. *science*, 316(5822):272–274, 2007.